Time-angle ocean acoustic tomography using sensitivity kernels: Numerical and experimental inversion results

Florian Aulanier, Barbara Nicolas, Philippe Roux, Romain Brossier, Jerome Mars

Proceedings of Meetings on Acoustics

Volume 19, 2013 http://acousticalsociety.org/

ICA 2013 Montreal
Montreal, Canada
2 - 7 June 2013

Acoustical Oceanography
Session 3pAO: Ocean Acoustical Tomography

3pAO3. Time-angle ocean acoustic tomography using sensitivity kernels: Numerical and experimental inversion results

Florian Aulanier*, Barbara Nicolas, Philippe Roux, Romain Brossier and Jérôme I. Mars

***Corresponding author's address: Departement Image Signal -- DIS, Grenoble Image Parole Signal Automatique -- GIPSA lab, 11 rue des Mathématiques, SAINT MARTIN D'HERES, 38402, Rhône-Alpes, France, Florian.Aulanier@gipsa-lab.grenoble-inp.fr**

In shallow water acoustic tomography, broadband mid-frequency acoustic waves (1 to 5 kHz) follow multiple ray-like paths to travel through the ocean. Travel-time (TT) variations associated to these raypaths are classically used to estimate sound speed perturbations of the water column using the ray theory. In this shallow water environment, source and receiver arrays, combined with adapted array processing, provide the measurement of directions-of-arrival (DOA) and directions-of-departure (DOD) of each acoustic path as new additional observables to perform ocean acoustic tomography. To this aim, the double-beamforming technique is used to extract the TT, DOA and DOD variations from the array-to-array acoustic records. Besides, based on the first order Born approximation, we introduce the time-angle sensitivity kernels to link sound speed perturbations to the three observable variations. This forward problem is then inverted with the maximum a posteriori method using both the extracted-observable variations and the proposed sensitivity kernels. Inversion results obtained on numerical data, simulated with a parabolic equation code, are presented. The inversion algorithm is performed with the three observables separately, namely TT, DOA and DOD. The three observables are then used jointly in the inversion process. The results are discussed in the context on ocean acoustic tomography.

Published by the Acoustical Society of America through the American Institute of Physics

 [DOI: 10.1121/1.4798965]
Received 19 Jan 2013; published 2 Jun 2013

INTRODUCTION

The concept of ocean acoustic tomography introduced by Munk and Wunsh in 1979 (1) aims at using acoustic wave propagation to retrieve seawater characteristics.

In shallow water waguides, mid-frequency acoustic wave take multiple ray-like paths to propagate from one point to another one (Fig. 1). The acoustic arrivals corresponding to each raypath can be identified by their travel-times (TT), direction-of-arrival (DOA) and direction-of-departure (DOD) as shown on Fig. 1.

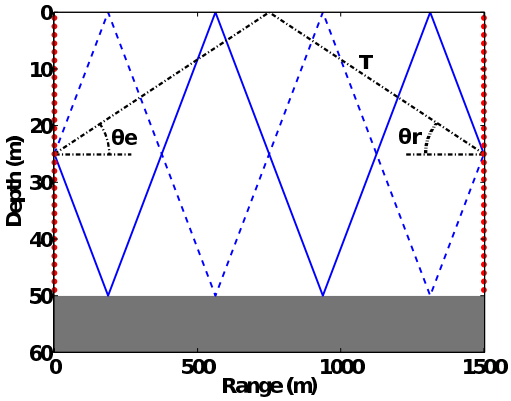

FIGURE 1: Pekeris waveguide with examples of three possible raypaths. The source and receive array at the beginning and the end of the waveguide have 97 elements evenly spaced by 0.5 m i.e. .These observables – measured with source-receiver arrays and the double beamforming technique (2; 3) – vary when the sound speed distribution changes in the waveguide.

In ocean acoustic tomography, TT have been classically used to retrieve waveguide sound speed maps (4; 5; 6). Indeed, when sound-speed perturbations occur in the waveguide, TT vary according to the size, the location and the value of the perturbation. Using source-receiver arrays and adapted signal processing (2; 3; 7; 8), it is possible to record DOA and DOD variations due to sound-speed perturbations as well. The relation between TT, DOA and DOD variations and sound speed perturbations can be approximated linearly using the sensitivity kernel theory(9; 10; 11).

In this paper, ocean acoustic tomography using jointly TT, DOA and DOD is performed. An inversion scheme using the maximum a posteriori (12; 13) and time-angle sensitivity kernels (T-A-SK) is presented in part 2, and then applied on numerical dataset obtained with parabolic equation simulations in part 3.

INVERSION OF THE T-A-SK FORWARD PROBLEM USING THE MAXIMUM A POSTERIORI

The formulation of the forward problem using the T-A-SK (11) – i.e. the mathematical link between the TT, DOA and DOD variations measured with double-beamforming, $\delta\tau$, $\delta\theta_r$, $\delta\theta_e$, and the sound-speed perturbation, δc – is expressed as:

$$\begin{pmatrix} \delta\tau \\ \delta\Theta_r \\ \delta\Theta_e \end{pmatrix} \simeq \iiint_V \begin{pmatrix} K_{TT}(\boldsymbol{r}') \\ K_{DOA}(\boldsymbol{r}') \\ K_{DOD}(\boldsymbol{r}') \end{pmatrix} \delta c(\boldsymbol{r}')\, \mathrm{d}V(\boldsymbol{r}') \tag{1}$$

where K_{TT}, K_{DOA} and K_{DOD} are the sensitivity kernels associated to each observable TT, DOA and DOD respectively. The waveguide volume is noted as V and $\mathrm{d}V(\boldsymbol{r}')$ is an elementary volume located in the waveguide at point $\boldsymbol{r}'$.

An example of T-A-SK is represented on Fig. 2 and shows the sensitivity of the acoustic path reflected twice on the surface and the bottom of the waveguide (plain line) for each observable.

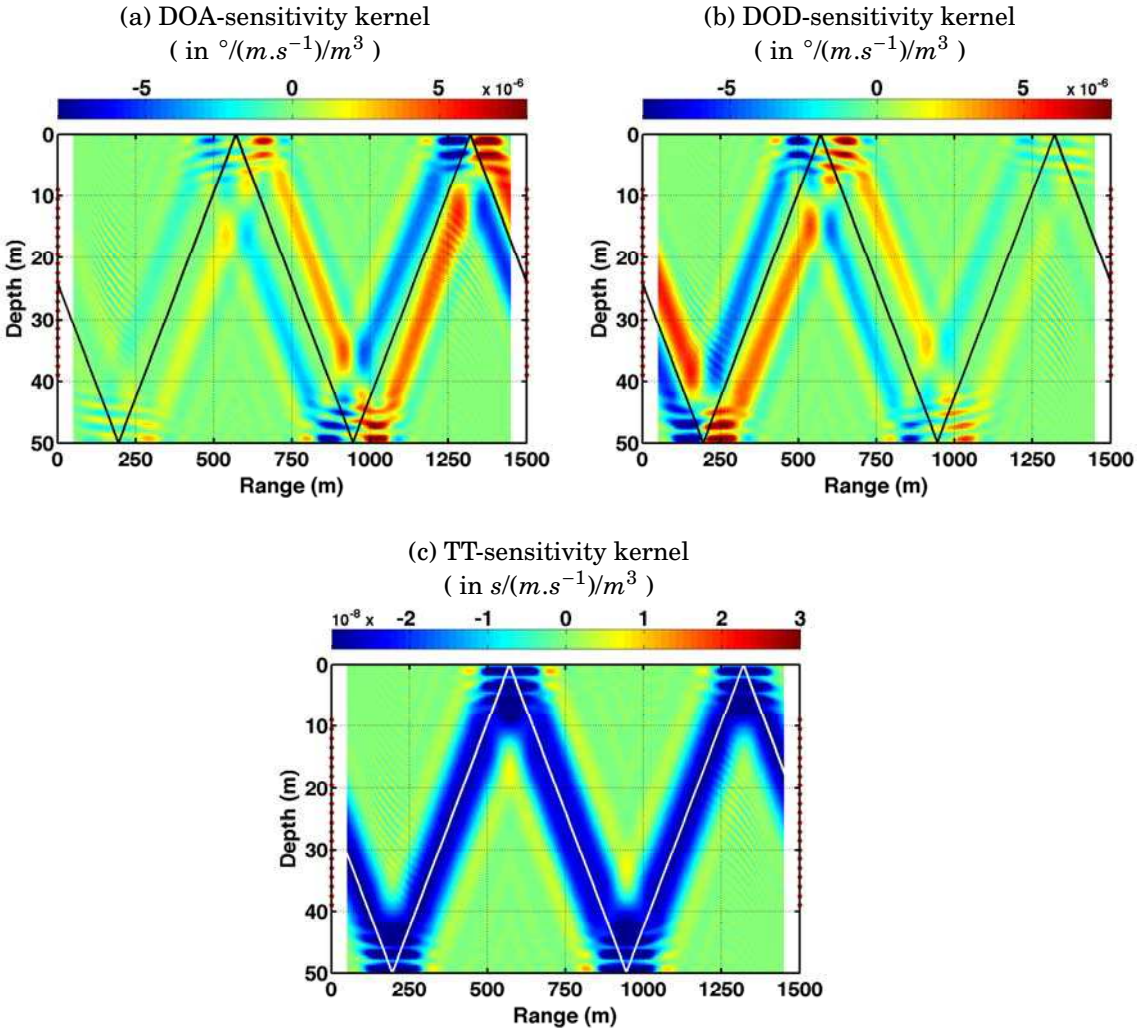

FIGURE 2: (a) DOA-, (b) DOD-, (c) TT-sensitivity kernel associated to the raypath shown in plain line. Positive (resp. negative) zones represent areas where a positive sound-speed perturbation induces a positive (resp. negative) variation of DOA, DOD or TT.

Then, this forward problem is inverted thanks to the maximum a posteriori method (12; 13). Assuming that data misfit and the model prior misfit are statistically gaussian, the maximum a posteriori can be written as:

$$\widehat{\boldsymbol{m}_{\boldsymbol{MAP}}} = \boldsymbol{m_0} + \lambda \boldsymbol{C_m} \boldsymbol{G}^T (\boldsymbol{G} \lambda \boldsymbol{C_m} \boldsymbol{G}^T + \boldsymbol{C_d})^{-1} (\boldsymbol{d} - \boldsymbol{G} \boldsymbol{m_0}) \tag{2}$$

Where $\boldsymbol{d}$ is the data vector (i.e. the TT, DOA and DOD variations of each acoustic arrival), $\boldsymbol{m}$ is the model vector (i.e. pixels of the sound-speed perturbation map) and $\boldsymbol{G}$ is Fréchet derivative matrix (i.e. matrix containing the T-A-SK). The prior knowledge is contained in $\boldsymbol{C_d}$, the data covariance matrix, $\boldsymbol{C_m}$, the model covariance matrix and $\boldsymbol{m_0}$, the model statistical mean. λ is the L-curve parameter included to adjust the importance of the model prior information relatively to the data information (14; 15).

Each observable is assumed to be independent which implies that $\boldsymbol{C_d}$ is diagonal. Because all the diagonal terms are not referring to the same observable, the relative weight between

observables is adjusted using prior information obtained on a training numerical set. Besides, it has been assumed that the sound-speed perturbation at a certain point of the waveguide is correlated with perturbation of the surrounding points. This spatial correlation has been assumed to be Gaussian, λ_r and λ_z being the parameters determining respectively the correlation lengths in range and depth. All this prior information is contained in the model covariance matrix, $\boldsymbol{C_m}$.

The theoretical part being presented, the natural follow up is to apply it on numerical simulation to see the results.

Inversion of a simulated dataset

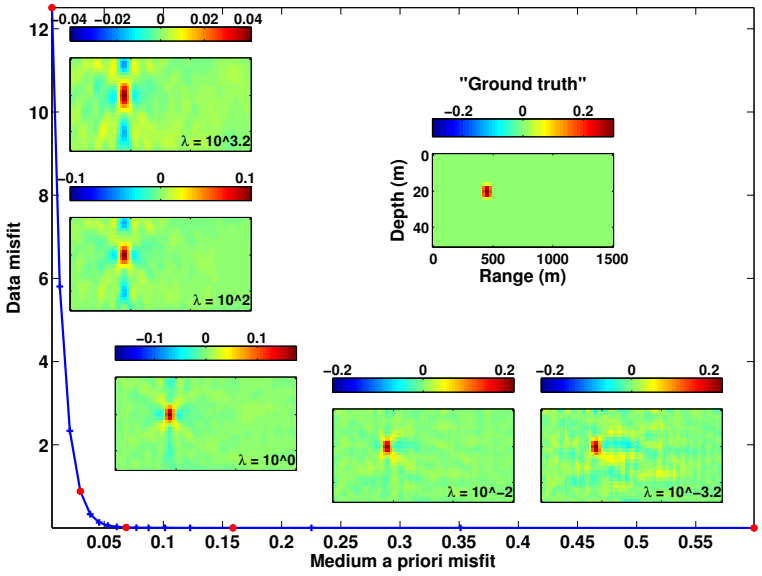

Figure 3: Inversion results for different values of lambda ($\lambda = 10^{3.2}$, 10^2, 1, 10^{-2}, $10^{-3.2}$) compared to the "ground truth" that is the sound-speed perturbation map used in the PE simulations.

In order to test the inversion using the T-A-SK, a set of two 3D-signals – in time, receiver depth, source depth – is simulated with a Padé parabolic equation code. The first signal is propagated in a uniform sound-speed (1500 m/s) Pekeris waveguide of 1500 m in length and 50 m in depth (see Fig. 1). And the second one, is propagated in the same waveguide with a sound-speed perturbation of 0.3 m/s (0.02% of the background) (see "ground truth" on Fig. 3). The 3D-signals are recorded on 25-pairs of source-receiver arrays of 21 meters in aperture (43 hydrophones). The signal is a Gaussian pulse with a bandwidth of 1.25 kHz centered on 2.5 kHz.

Observables are extracted out of these signals for 550 raypaths with 2 to 12 reflections on the seafloor and the sea surface. Variations of each observable are computed and used to retrieve the sound-speed perturbation map.

Results are shown on the Fig. 3 for different values of lambda. The L-curve (14; 15) represented in plain line on Fig. 3 shows that the highest values of lambda allow a better fit to the data whereas lower values of lambda constrain the inversion to tend toward the medium prior. The best inversion result is then found close to the ($\lambda = 1$) when a trade-off is found between data fit and a medium prior fit. Indeed, by giving more weight to the data, the maximum value of the perturbation is closer to the "ground truth" one. However, giving more weight to the medium prior reduces the background noise level.

This gives good inversion results regarding the perturbation shape and the background noise, in spite of the fact that the perturbation value is only retrieved at 50% of what it should be. Other scenarios with different locations of the perturbation have also been tested giving the same results. This shows that the T-A-SK inversion results do not depend on the location of the perturbation regarding the source/receiver arrays.

Conclusion

For the first time in ocean acoustic tomography, a sound-speed perturbation has been retrieved using directions-of-arrival and directions-of-departure of acoustic wavepaths, jointly with their corresponding travel-times. This has been done thanks to double-beamforming array processing, time-angle sensitivity kernels and maximum a posteriori inversion. Further investigations should lead to perform underwater acoustic inversions on small-scale experiment data, to see if the time-angle sensitivity kernels can be used to retrieve sound-speed perturbations occurring in real environments.

Acknowledgements

The authors would like to acknowledge to Dr. J. Sarkar and Dr. B. Cornuelle from the Marine Physical Laboratory, SIO for their help on PE simulations and their useful discussions; and Dr. E. Skarsoulis from the Institute of Applied and Computational Mathematics, FORTH for his helpful comments.

References

[1] W. Munk and C. Wunsch, “Ocean acoustic tomography: a scheme for large scale monitoring”, Deep Sea Research Part A. Oceanographic Research Papers **26**, 123–161 (1979).

[2] P. Roux, B. D. Cornuelle, W. A. Kuperman, and W. S. Hodgkiss, “The structure of raylike arrivals in a shallow-water waveguide.”, The Journal of the Acoustical Society of America **124**, 3430–9 (2008).

[3] B. Nicolas, I. Iturbe, P. Roux, and J. Mars, “Double formation de voies pour la séparation et l’identification d’ondes: applications en contexte fortement bruité et à la campagne faf03”, TS. Traitement du signal **25**, 293–304 (2008).

[4] W. Munk and C. Wunsch, “Observing the ocean in the 1990s”, Philosophical Transactions of the Royal Society of London. Series A, Mathematical and Physical Sciences **307**, 439–464 (1982).

[5] B. Howe, P. Worcester, and R. Spindel, “Ocean acoustic tomography: Mesoscale velocity”, J. Geophys. Res **92**, 3785–3805 (1987).

[6] B. Cornuelle and B. Howe, “High spatial resolution in vertical slice ocean acoustic tomography”, J. Geophys. Res **92**, 680–11 (1987).

[7] L. Jiang, F. Aulanier, G. Le Touzé, B. Nicolas, and J. Mars, “Raypath separation with high resolution processing”, in *OCEANS, 2011 IEEE-Spain*, 1–5 (IEEE) (2011).

[8] G. Le Touzé, B. Nicolas, J. Mars, P. Roux, and B. Oudompheng, “Double-capon and double-musical for arrival separation and observable estimation in an acoustic waveguide”, EURASIP Journal on Advances in Signal Processing (To be published).

[9] E. K. Skarsoulis and B. D. Cornuelle, “Travel-time sensitivity kernels in ocean acoustic tomography”, Journal of the Acoustical Society of America **116**, 228–238 (2004).

[10] I. Iturbe, P. Roux, B. Nicolas, J. Virieux, and J. I. Mars, “Shallow-Water Acoustic Tomography Performed From a Double-Beamforming Algorithm: Simulation Results”, IEEE Journal of Oceanic Engineering **34**, 140–149 (2009).

[11] F. Aulanier, B. Nicolas, P. Roux, and J. I. Mars, “Direction-of-arrival, direction-of-departure and travel-time sensivity kernels obtained through double beamforming in shallow water”, in *Proceedings of the 4th international conference and exhibition on Underwater Acoustic Measurements: Technologies and Results*, volume 4, 453–460 (2011).

[12] J. Melsa and D. Cohn, *Decision and estimation theory*, volume 4 (McGraw-Hill New York:) (1978).

[13] A. Tarantola, *Inverse problem theory and methods for model parameter estimation* (Society for Industrial Mathematics) (2005).

[14] P. Hansen, “Analysis of discrete ill-posed problems by means of the l-curve”, SIAM review **34**, 561–580 (1992).

[15] P. Hansen and D. O’Leary, “The use of the l-curve in the regularization of discrete ill-posed problems”, SIAM Journal on Scientific Computing **14**, 1487–1503 (1993).